Organic Electronics 14 (2013) 762–767

Contents lists available at SciVerse ScienceDirect

Organic Electronics

journal homepage: www.elsevier.com/locate/orgel

Low threshold melt-processed two-photon organic surface emitting upconversion lasers

Hong-Hua Fang [a], Shi-Yang Lu [b], Xue-Peng Zhan [a], Jing Feng [a,*], Qi-Dai Chen [a], Hai-Yu Wang [a,*], Xing-Yuan Liu [c,*], Hong-Bo Sun [a,b,*]

[a] State Key Laboratory on Integrated Optoelectronics, College of Electronic Science and Engineering, Jilin University, 2699 Qianjin Street, Changchun 130012, China
[b] College of Physics, Jilin University, 119 Jiefang Road, Changchun 130023, China
[c] State Key Laboratory of Luminescence and Applications, Changchun Institute of Optics, Fine Mechanics and Physics, Chinese Academy of Sciences, Changchun 130033, China

ARTICLE INFO

Article history:
Received 22 October 2012
Received in revised form 23 November 2012
Accepted 14 December 2012
Available online 29 December 2012

Keywords:
Organic semiconductor
Two-photon
Upconversion
Distributed bragg reflector
Melt-process

ABSTRACT

Herein, a low threshold, wavelength-tunable, compact, two-photon pumped upconversion laser is presented. The surface emitting lasers are composed of melt-processed 1,4-bis[2-[4-[N,N-di(*p*-totyl)amino]phenyl]vinyl]benzene (DADSB) as active media and two designed distributed bragg reflectors. The melting fabrication process is very simple, and the lasing threshold is as low as 150 μJ cm^{-2} $pulse^{-1}$, when pumped by a Ti:sapphire amplifier operating at 800 nm with a 150 fs pulse width. To the best of our knowledge, it is one of the lowest values for two-photon lasers. Lasing from multimode to single-mode oscillation is demonstrated. Tunable single mode oscillation was obtained at wavelength from 514 nm to 523 nm with a spectral width of less than 0.2 nm.

1. Introduction

Organic gain media have shown great potential applications in different photonic devices, such as light-emitting sources, switchers, lasers and optical amplifiers [1–7]. In particular, the properties of organic materials could be tailored to allow for novel approaches to make laser devices. Two-photon absorption (2PA) has attracted great attentions for fluorescence imaging and 3D microfabrication [8–10]. In 2PA process, two photons of lower energy (longer wavelength) can be used to bridge the energy gap of the material instead of one high-energy (short wavelength) photon, and it allows for optical absorption to occur in a spectral range where the single-photon absorption is negligible [11]. Then, IR radiation can be absorbed by a material that emits higher energy photon. It provides an alternative approach to accomplish one kind of novel laser devices, which is called two-photon pumped (TPP) laser. Unlike second harmonic generation, phase-matching requirement is not required [12–14] and it allows using near-IR solid-state pump sources, which are cheaper and more compact, compared to the UV versions. Hence, great efforts have been made to explore the two-photon pumped laser devices [14–20].

For applications, it is quite necessary to develop lasers with low threshold, especially for two-photon excitation. The lower excitation intensity makes the degradation process slower and possible laser operation in the high-repetition rate regime. High pump intensity is generally required for TPP lasing purposes, because of the much-lower-absorption cross-section and actually, a small portion of the incident light is absorbed. To address this problem, it would be desirable to utilize high-density molecules with large TPA cross section in active media to harvest pump light as more as possible. It is demonstrated that low threshold amplified spontaneous emission can

* Corresponding author at: State Key Laboratory on Integrated Optoelectronics, College of Electronic Science and Engineering, Jilin University, 2699 Qianjin Street, Changchun 130012, China.
E-mail addresses: jingfeng@jlu.edu.cn (J. Feng), xingyuanliu@hotmail.com (X.-Y. Liu), hbsun@jlu.edu.cn (H.-B. Sun).

1566-1199/$ - see front matter © 2013 Elsevier B.V. All rights reserved.
http://dx.doi.org/10.1016/j.orgel.2012.12.019

be realized in organic single crystals, in which the chromophore density is extremely high [21–23]. The TPP lasing threshold is only one order larger than that pumped by single-photon pumping [23]. However, organic single crystals have been limited to fundamental studies, because the fabrication of single crystal laser devices poses a technological challenge [24].

In the present work, we report melt-processed two-photon surface emission laser. The material exhibits a low temperature melting point, which allows the fabrication of laser device feasible, especially for mass production. Meantime, the melt-processed method ensures enough high chromophore density in active media. Two-photon pumped upconversion lasing with a threshold as low as of 150 μJ pulse^{-1} cm^{-2} was achieved upon pumped with near-IR (800 nm) radiation. The cavity length of laser could be easily tuned, and lasing oscillation from multimode to single mode was realized.

2. Experimental

2.1. Thermal properties of materials

The active material used here is 1,4-bis[2-[4-[N,N-di(p-totyl)amino]phenyl]vinyl]benzene (DADSB), whose molecular structure is shown in Fig. 1a. The melting experiment was carried out in glove box with dry nitrogen gas. The powder of materials was mounted on the hot stage and heated, and molten on a glass slide as the substrate, through the medium of an iron plate. The temperature of the hot stage was regulated typically using a thermocouple around a desired temperature. The morphology of materials can easily be examined by eyesight or under microscope. The thermal property of materials was further investigated by differential scanning calorimetric (DSC) measurement, which was performed on a NETZSCH DSC204 instrument. Thermogravimetric analyses (TGA) were performed on a TA Q500 thermogravimeter for evaluation of their thermal stability.

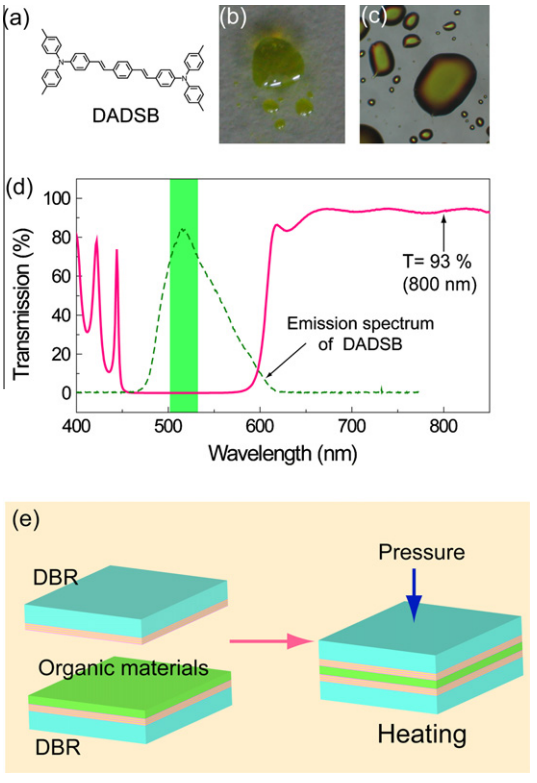

Fig. 1. (a) Molecular structure of DADSB. (b) Image of liquid DADSB. (c) Liquid DADSB drop under investigated under microscope. (d) Experimental transmitting spectrum of distributed bragg reflector at near-normal incidence and two-photon excited emission spectra (dot line) excited by 800 nm. (e) Schematic diagram of fabrication process of surface emitting laser.

2.2. Device fabrication

The laser microcavity fabrication process is shown in Fig. 1e. Firstly, powder materials were spread on a DBR with a spatula. Then, another DBR was covered onto the powder. The two DBRs were stacked together with the help of a hold-down plate in a face-to-face fashion and horizontally placed into a small chamber in glove box. Thirdly, the double-DBRs were heated slowly at temperature above melt point and held for 5 min. Upon melting in a nitrogen atmosphere, application of pressure caused liquid DADSB filled in the microcavity. The two surfaces of DBRs were adjusted to be parallel, as much as possible. Then the sample was moved from the heated chamber and cooled slowly to

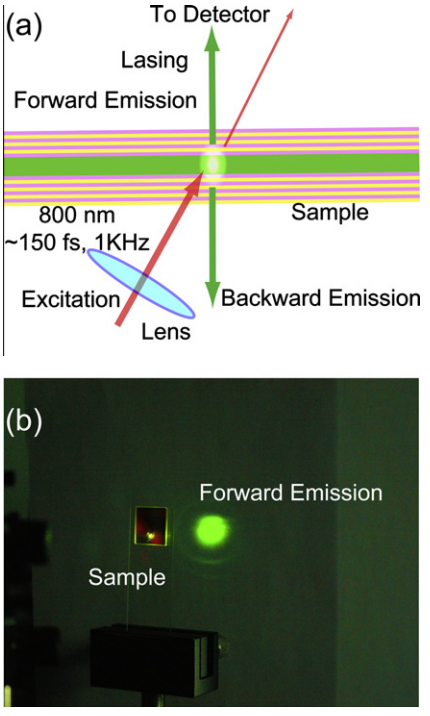

Fig. 2. (a) Schematic of the experimental setup for measuring the lasing output. (b) Photograph of the green lasing (~520 nm) from the laser structure. A highly directional lasing output in the forward direction was observed on a white background. The pump wavelength is 800 nm. (For interpretation of the references to color in this figure legend, the reader is referred to the web version of this article.)

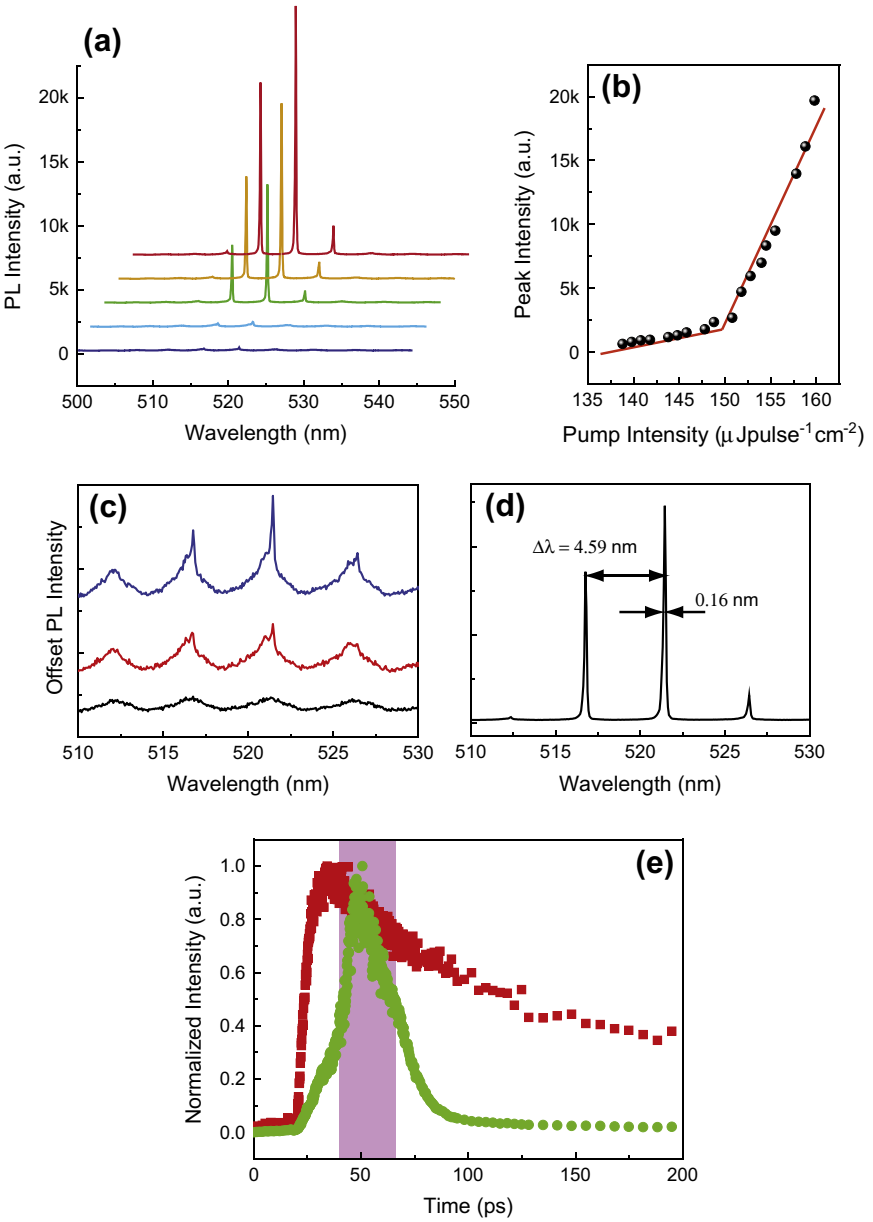

Fig. 3. (a) PL spectra form the laser device pumped at different intensities. (b) Peak intensity vs. pump intensity, the threshold is about 150 μJ cm^{-2} $pulse^{-1}$. Enlarged PL spectra (c) near the threshold and (d) above the threshold. (e) Photoluminescence dynamics investigated by time-resolved upconversion technique near the threshold and above threshold.

room temperature. The materials would fill and solidify in microcavity.

2.3. Optical characterization

UV–vis absorption spectra were recorded on a UV-3100 spectrophotometer. Fluorescence was measured with a RF-5301PC spectrofluorimeter. For measurement of two-photon absorption cross section, a tunable Ti:Sapphire laser system delivering 150 fs pulses at 76 MHz repetition rate was used. Solution of fluorescein in water at pH ~ 11 (0.1 mol/L NaOH) was used as a reference standard [25].

2.4. Characterization of lasing performance

The fundamental frequency of output from a Ti:sapphire amplifier laser (λ = 800 nm, pulse width = 150 fs, repetition rate = 1 kHz) was used as an excitation source. The pump laser beam was focused onto the sample with a 2.54-cm-diameter lens of 60 cm focal length and at an incidence angle of 20° from the normal to the sample surface, giving a beam diameter at the sample of about 1 mm. The resulting emission was collected via an optical fiber coupled to a spectrometer and detected by a charge coupled device (CCD) camera.

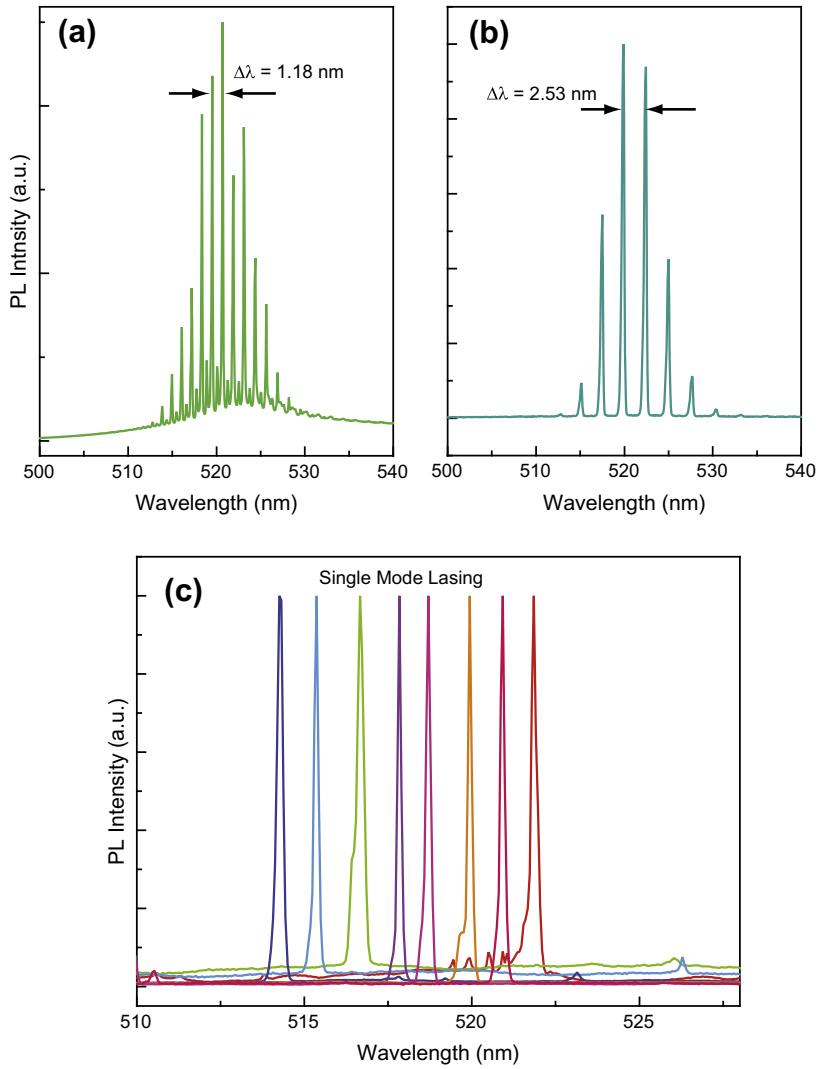

Fig. 4. (a and b) Multimode lasing spectra from devices with different thickness. Mode spacing and position can be tuned by the thickness. (c) Single-mode lasing spectra from device, the wavelength were tuned from 510 nm to 523 nm.

2.5. Time-resolved fluorescence upconversion measurement

The pulse from the Ti:sapphire regenerative amplifier with laser pulse of 800 nm, ~150 fs optical pulse duration, and 1 kHz repetition rate is split into two parts. One is focused onto the sample to excite laser emission; the other is sent into an optical delay line and serves as the gate pulse. The emission light from the sample was collected by an off-axis parabolic mirror and focused on the beta-bariumborate (BBO) crystal. The generated sum frequency light was then collimated and focused into the entrance slit of a 300 mm monochromatic, spectrally resolved, and detected by a photomultiplier tube.

3. Results and discussions

The DADSB melt when it was heated to a certain temperature. Fig. 1b illustrates an image of liquid DADSB droplets at temperature of 240 °C, while Fig. 1c shows small size cooled dropt under microscopy at room temperature. Changes of visual appearance are ascribed to the formation of an isotropic melt. It then makes us possible to let the materials melted into predefined geometry channels and let the material solidified for device applications. The thermal properties of DADSB were further studied as a function of thermal history by differential scanning calorimetry (DSC). The DSC result shows that there is a well-defined exothermic transition with a considerable enthalpy around 164 °C (corresponds to the crystallization of the sample) and melting transition at 225 °C (see Fig. S1, Supplementary data). The oligomer exhibits high thermal stability with decomposition temperatures more than 400 °C under nitrogen according to the further thermogravimetric analysis (Fig. S2, Supplementary data), which allows melt processing of DADSB materials without decomposition.

The melt-processed thin film exhibits very strong fluorescence when excited by fundamental harmonic emission

(150 fs, 800 nm) from amplifier, implying possibility for laser applications. Fig. 1d illustrates the two photon excitation fluorescence spectra, which is identical to that pumped by 405 nm lasers. According to the Kasha rule, in both cases the emission state is the same [26]. The 800 nm excited fluorescence intensity as a function of the incident energy shows a square dependence (Fig. S3, Supplementary data), which implies that the upconverted emission indeed stems from the two-photon-absorption mechanism. The TPA cross-section at 800 nm is determined to be 120 GM (1 GM = 10^{-50} cm^4 s photon^{-1} molecule^{-1}).

The laser device structure, shown in Fig. 1e, is composed of DADSB organic materials sandwiched between two distributed bragg reflectors (DBRs). The DBRs are intensively designed to be high transmission at the wavelength (800 nm), and low transmission from 480 to 570 nm as shown in Fig. 1d. So it is possible for the devices to be pumped by 800 nm pulsed lasers, i.e. two-photon excitation.

The lasing performance is evaluated with configuration as shown in Fig. 2a. As the average power of the excitation pulse increased above the lasing threshold, well-defined lasing beam was vertically emitted from the surface of the sample in both the forward and backward directions. Highly directional emission pattern from the sample surface was observed when the pump power exceeded a certain value (Fig. 2b).

The room temperature photoluminescence (PL) spectra at different excitation pump intensities are illustrated in Fig. 3a. Above the lasing threshold, sharp lasing peaks occur at around 520 nm. A typical plot of output intensity in the forward direction versus input intensity is shown in Fig. 3b. They show the typical signatures of laser action, namely a clear threshold at about 150 μJ cm^{-2} pulse^{-1} for this sample, which is of a magnitude about one-tenth of previously reported values for two-photon pumped polyfluorene laser [27]. To the best of our knowledge, it is one of the lowest threshold lasers for two-photon lasing [16,27,28]. The total lasing output energy at input intensity of 1.26 mJ, corresponding to 160 μJ cm^{-2} pulse^{-1}, was 60 μJ. Therefore, the overall energy conversion efficiency from the input to the output was about 5% for this sample at this pump level.

To further investigate the lasing mechanism clearly, PL spectrum recorded near and above threshold have been enlarged and presented in Fig. 3c and d, respectively. Obvious constructive interference in emission spectrum could be seen at low pump intensity (Fig. 3c). When the pump is high enough, a clear sharp emission line with the linewidth about 0.16 nm was observed. The mode spacing of the lasing denoted as $\Delta\lambda$ is measured to be 4.59 nm. Let d and n be the thickness and the effective refractive index of a *F–P* cavity, respectively, the resonant condition can be approximately written as $2nd = N\lambda$, where N is the mode number and λ is resonant wavelength. Thus, the expected mode spacing, $\Delta\lambda$, is given by $\Delta\lambda = \lambda^2/2n_g d$, n_g is a group refractive index [29,30]. According to the measured mode spacing, and $n_g \sim 1.7$, the thickness of DADSB for this sample is about 17 μm. The temporal profiles of the forward-stimulated emission from the device were further investigated utilizing a time-resolved fluorescence upconversion technique [31]. Fig. 3e shows the normalized temporal profiles for the TPA-induced emission observed from one device at two different pump energies, 130 and 155 μJ cm^{-2} pulse^{-1}, where the monitor wavelength corresponded to the peak position of time-integrated spectra. Under low-intensity excitation, the emission shows a slow decay characteristic, while the emission decay time is dramatically shortened to be 23 ps as pump intensity increased.

The lasing wavelength is tuned when the thickness of melted DADSB film is changed, which can be controlled by adjusting pressure added on the DBRs during the melt process. As indicated in Fig. 4a and b, multimode lasing spectra with different frequency spacing and number is presented. Frequency spacing becomes larger as the thickness decrease, and single mode lasing can be achieved if the frequency spacing from the cavity is comparable to the width of the lasing region [30]. Following this idea, we have indeed observed single mode lasing. The curves in Fig. 4c depict the selected lasing emission with wavelength from 514 to 523 nm. The spectrum was captured under pump intensity above the threshold. It can be seen that the lasing action is entirely occupied by a single mode, which indicates the tunability of the proposed two-photon lasers.

4. Conclusions

To summarize, we have presented the fabrication of two-photon pumped upconversion organic lasers with a simple and feasible technique. Tunable upconversion surface emitting multimode and single-mode lasing were observed from the laser cavities at room temperature. The presented laser cavities exhibit a very low threshold and an ultrafast pulse emission. Owing to the simple, low threshold, our system offers a versatile candidate for the future application of frequency upconversion as well as other photonic devices.

Acknowledgement

This work was supported by the Natural Science Foundation of China (NSFC) under Grants #90923037, 61137001 and 61127010.

Appendix A. Supplementary material

Supplementary data associated with this article can be found, in the online version, at http://dx.doi.org/10.1016/j.orgel.2012.12.019.

References

[1] C. Grivas, M. Pollnau, Laser Photonics Rev. 6 (2012) 419–462.
[2] Y.J. Chen, J. Herrnsdorf, B. Guilhabert, A.L. Kanibolotsky, A.R. Mackintosh, Y. Wang, R.A. Pethrick, E. Gu, G.A. Turnbull, P.J. Skabara, I.D.W. Samuel, N. Laurand, M.D. Dawson, Org. Electron. 12 (2011) 62–69.
[3] M. Lehnhardt, T. Riedl, U. Scherf, T. Rabe, W. Kowalsky, Org. Electron. 12 (2011) 1346–1351.
[4] S. Hotta, T. Yamao, J. Mater. Chem. 21 (2011) 1295–1304.

[5] M. Muccini, W. Koopman, S. Toffanin, Laser Photonics Rev. 6 (2012) 258–275.
[6] E. Matioli, S. Brinkley, K.M. Kelchner, Y.L. Hu, S. Nakamura, S. DenBaars, J. Speck, C. Weisbuch, Light Sci. Appl. 1 (2012) e22, http://dx.doi.org/10.1038/lsa.2012.22.
[7] S. Seo, Y. Kim, J. You, B.D. Sarwade, P.P. Wadgaonkar, S.K. Menon, A.S. More, E. Kim, Macromol. Rapid Commun. 32 (2011) 637–643.
[8] S.H. Park, D.Y. Yang, K.S. Lee, Laser Photonics Rev. 3 (2009) 1–11.
[9] G.S. He, L.S. Tan, Q.D. Zheng, P.N. Prasad, Chem. Rev. 108 (2008) 1245–1330.
[10] W. Xiong, Y.S. Zhou, X.N. He, Y. Gao, M. Mahjouri-Samani, L. Jiang, T. Baldacchini, Y.F. Lu, Light Sci. Appl. 1 (2012) e6, http://dx.doi.org/10.1038/lsa.2012.1036.
[11] M. Pawlicki, H.A. Collins, R.G. Denning, H.L. Anderson, Angew. Chem. Int. Ed. 48 (2009) 3244–3266.
[12] Y.R. Shen, The Principles of Nonlinear Optics, John Wiley & Sons, New York, 1984.
[13] C. Bauer, B. Schnabel, E.B. Kley, U. Scherf, H. Giessen, R.F. Mahrt, Adv. Mater. 14 (2002) 673–676.
[14] Q. Chen, C.F. Zhang, B. Jiang, X.Y. Wang, Y.J. Liu, Y. Cao, M. Xiao, Opt. Express 20 (2012) 9135–9143.
[15] G.S. He, T.C. Lin, V.K.S. Hsiao, A.N. Cartwright, P.N. Prasad, L.V. Natarajan, V.P. Tondiglia, R. Jakubiak, R.A. Vaia, T.J. Bunning, Appl. Phys. Lett. 83 (2003) 2733–2735.
[16] F. Scotognella, D.P. Puzzo, M. Zavelani-Rossi, J. Clark, M. Sebastian, G.A. Ozin, G. Lanzani, Chem. Mater. 23 (2011) 805–809.
[17] C. Zhang, C.L. Zou, Y.L. Yan, R. Hao, F.W. Sun, Z.F. Han, Y.S. Zhao, J.N. Yao, J. Am. Chem. Soc. 133 (2011) 7276–7279.
[18] G. Tsiminis, J.-C. Ribierre, A. Ruseckas, H.S. Barcena, G.J. Richards, G.A. Turnbull, P.L. Burn, I.D.W. Samuel, Adv. Mater. 20 (2008) 1940–1944.
[19] K.D. Belfield, M.V. Bondar, C.O. Yanez, F.E. Hernandez, O.V. Przhonska, J. Mater. Chem. 19 (2009) 7498–7502.
[20] K. Shirota, H.B. Sun, S. Kawata, Appl. Phys. Lett. 84 (2004) 1632–1634.
[21] Q.D. Chen, H.H. Fang, B. Xu, J. Yang, H. Xia, F.P. Chen, W.J. Tian, H.B. Sun, Appl. Phys. Lett. 94 (2009) 201113.
[22] H.H. Fang, Q.D. Chen, J. Yang, H. Xia, Y.G. Ma, H.Y. Wang, H.B. Sun, Opt. Lett. 35 (2010) 441–443.
[23] H. Xia, J. Yang, H.H. Fang, Q.D. Chen, H.Y. Wang, X.Q. Yu, Y.G. Ma, M.H. Jiang, H.B. Sun, Chem. Phys. Chem. 11 (2010) 1871–1875.
[24] H.H. Fang, R. Ding, S.Y. Lu, J. Yang, X.L. Zhang, R. Yang, J. Feng, Q.D. Chen, J.F. Song, H.B. Sun, Adv. Funct. Mater. 22 (2012) 33–38.
[25] C. Xu, W.W. Webb, J. Opt. Soc. Am. B 13 (1996) 481–491.
[26] J.R. Lakowicz, Principles of Fluorescence Spectroscopy, third ed., Springer, Singapore, 2006.
[27] G. Tsiminis, A. Ruseckas, I.D.W. Samuel, G.A. Turnbull, Appl. Phys. Lett. 94 (2009) 253304.
[28] W. Li, C.F. Zhang, Q. Chen, X.Y. Wang, M. Xiao, Appl. Phys. Lett. 100 (2012).
[29] H.H. Fang, R. Ding, S.Y. Lu, Y.D. Yang, Q.D. Chen, J. Feng, Y.Z. Huang, H.B. Sun, Laser Photonics Rev. 5 (2012), http://dx.doi.org/10.1002/lpor.201200072.
[30] O. Svelto, Principles of Lasers, fifth ed., Springer, New York, 2009.
[31] H.H. Fang, Q.D. Chen, R. Ding, J. Yang, Y.G. Ma, H.Y. Wang, B.R. Gao, J. Feng, H.B. Sun, Opt. Lett. 35 (2010) 2561–2563.